

# Magneto Hydrodynamic Flow of Dissipative Non-Newtonian Fluid over an Exponential Stretching Surface with Thermal Radiation

M.Sailaja<sup>1</sup> R.Hemadri Reddy<sup>2</sup>

1.Department of Mathematics, Dravidian University, Kuppam-517425, India

2.Department of Mathematics, VIT University, Vellore - 632014, India

## Abstract

Numerical investigation is carried out to analyze the flow, heat and mass transfer behavior of magnetohydrodynamic non-Newtonian fluid (Casson) over a stretched surface with thermal radiation, chemical reaction and viscous dissipation effects. The governing PDEs are transformed as ODEs with the help of suited similarity transform. The effective Matlab package bvp5c is used to obtain the numerical solutions of the transformed equations. The impact of pertinent parameters on the common profiles (flow, temperature and concentration) is discussed in detail with the assistance of graphical illustrations for Casson and Newtonian fluid cases. Tabular results are presented to explain the nature of the wall friction, local Nusselt and Sherwood numbers.

**Keywords:** Magnetohydrodynamics; Radiation; Dissipation; Casson; Chemical reaction.

## 1. Introduction

Flow, heat and mass transfer investigation of non-Newtonian fluids is an area of great attention among the modern researchers. It is due to the potential applications in technology and industrial sectors. The biological and industrial fluids such as printer ink, liquid detergents, paints, sauce, polymers, multigrade oil, mud, etc. are the non-Newtonian fluids. Such fluids have amazing contribution in the fermentation, bubble absorption, devolatilisation, composite processing, bubble columns etc. AboEldahab [1] investigated the heat transfer characteristics of free convection MHD flow past a stretching sheet with radiation and buoyancy effects. The influence of thermal radiation on MHD Casson fluid flow over an exponentially stretching surface is presented by Pramanik [1]. Affify [3] explained the mass transfer and free stream flow over a vertical surface with radiation effect.

The influence of thermal conductivity on MHD steady incompressible flow past a stretching sheet was studied by Animasaun [4] and found that rising values of thermal conductivity enhances the temperature field. The numerical investigation of MHD heat transfer flow towards a stretching surface was analysed by Mukhopadhyay [5]. Sajid and Hayat [6] considered the MHD boundary layer flow towards a stretching surface. The effect of thermophoresis and Brownian motion on MHD boundary layer flow past a stretching surface was discussed by Ibrahim et al. [7] and solved numerically by R-K with shooting method. Raju et al. [8] reported the mass and heat transfer flow in MHD non-Newtonian fluid towards a stretching sheet with viscous dissipation and chemical reaction effects. Krishnamurthy et al. [9] investigated the 2D incompressible Williamson fluid flow with chemical reaction effect and concluded that increasing values of permeability parameter depreciate the velocity field. The three dimensional MHD non-Newtonian fluid flow towards a linearly stretching surface was studied by Mahanta and Shaw [10].

Gireesha et al. [11] discussed the 2D MHD boundary layer flow past a stretching surface in the presence of melting effect and numerically solved by shooting technique. The chemically reflex species in non-Newtonian fluid flow towards a stretching surface with magnetic field effect was studied by Hayat et al. [12]. Hayat et al. [13] analysed the influence of viscous dissipation on MHD nanofluid flow past a stretching cylinder by considering the variable properties. The steady incompressible free convective MHD non-Newtonian fluid flow towards a stretching sheet with heat generation/absorption and suction effects was considered by Animasaun et al. [14] and analytically solved by HAM technique. Ramana Reddy et al. [15] addressed the mass and heat transfer in Casson fluid past a sladering stretching surface by considering the magnetic field effect. The effect of melting and thermal radiation on MHD heat transfer flow over a stretching cylinder was reported by Hayat et al. [16].

Nadeem et al. [17] considered the 3D MHD non-Newtonian fluid flow over a linearly stretching surface and found that rising values of stretching parameter depreciate the velocity field. The MHD stagnation point flow of non-Newtonian fluid past a stretching sheet with Joule heating and viscous dissipation was investigated by Khan et al. [18]. Hayat et al. [19] reported the mass and heat transfer on MHD viscous flow through a porous medium towards a radiating stretching surface. The study of radiative MHD heat transfer of non-Newtonian fluid towards different geometries with nonlinear thermal radiation effect was pioneered by Ali and Sandeep [20]. Sathish Kumar et al. [21] discussed the influence of Cattaneo-Christov model on MHD Casson fluid flow past stretching sheet in the presence of nonlinear radiative effect and found that the Casson parameter have tendency to decreases friction factor. The MHD flow of non-Newtonian fluid over a stretched cylinder with Joule heating

and viscous dissipation effects was analysed by Tamoor et al. [22]. The analytical and numerical investigation of mass and heat transfer in Casson fluids towards different geometries was addressed by [23-30].

In this study, we analysed the mass and heat transfer in MHD flow of Casson fluid over an exponential stretching sheet with thermal radiation and chemical reaction effects. Further, graphical illustrations has been specified to study the influence of different pertinent parameters on flow, temperature and concentration profiles. Also, geometrical computations has been conceded to analyse the effect of different pertinent parameters presented in the flow on friction factor, local Nusselt and Sherwood numbers.

## 2. Mathematical Formulation

The 2D steady flow of Casson fluid over an exponential and a flat stretched surfaces is considered in such a way that the  $x$ -axis is located along the surface and  $y$  axis is normal to it. A transverse magnetic field  $B(x)$  is applied along  $y$  direction as displayed in Fig.1. Viscous dissipation, chemical reaction and thermal radiation effects are taken into an account. It is assumed that  $T$  and  $T_\infty$  are the surface and ambient temperatures and  $C$  and  $C_\infty$  are the surface and ambient concentration.

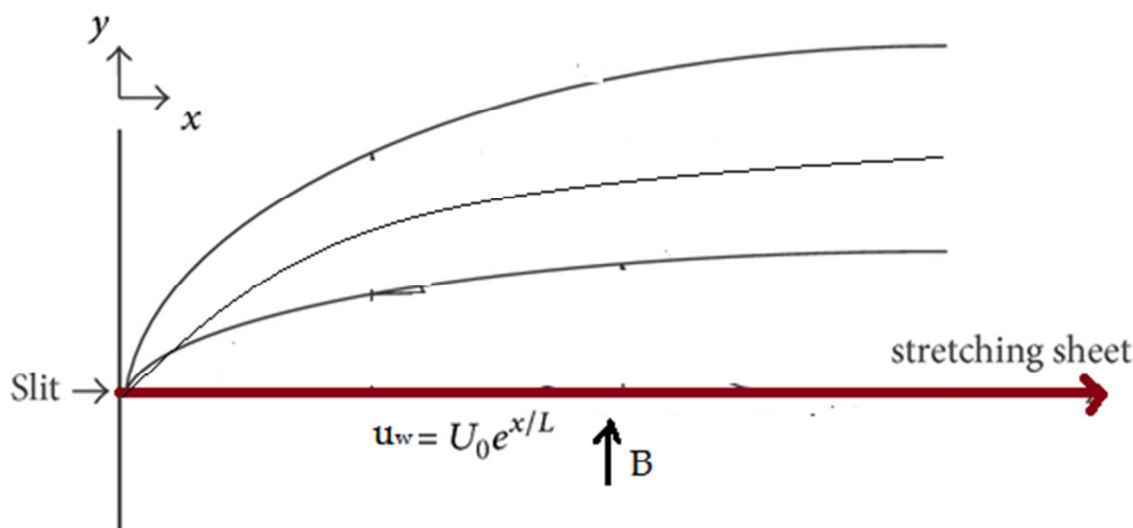


Fig.1 Physical model of the problem

The magnetic field induced by the electric field is ignored in this study. The boundary layer equations as per the assumptions given above can be express as:

$$\frac{\partial u}{\partial x} + \frac{\partial v}{\partial y} = 0 \quad (1)$$

$$u \frac{\partial u}{\partial x} + v \frac{\partial u}{\partial y} = \frac{1}{\rho} \left( \mu \left( 1 + \frac{1}{\delta} \right) \frac{\partial^2 u}{\partial y^2} + g(\rho\beta)(T - T_\infty) + g(\rho\beta^*)(C - C_\infty) - \sigma B^2(x)u \right), \quad (2)$$

$$u \frac{\partial T}{\partial x} + v \frac{\partial T}{\partial y} = \alpha \frac{\partial^2 T}{\partial y^2} + \frac{\mu}{(\rho c_p)} \left( \frac{\partial u}{\partial y} \right)^2 + \frac{16\sigma_1 T_\infty^3}{3(\rho c_p)_{nf} \chi} \frac{\partial^2 T}{\partial y^2}, \quad (3)$$

$$u \frac{\partial C}{\partial x} + v \frac{\partial C}{\partial y} = D_m \frac{\partial^2 C}{\partial y^2} - k_r (C - C_\infty), \quad (4)$$

With the boundary conditions

$$\left. \begin{aligned} u = u_w(x), v = 0, T = T_w, C = C_w \text{ at } y = 0 \\ u \rightarrow 0, T \rightarrow T_\infty, C \rightarrow C_\infty \text{ as } y \rightarrow \infty \end{aligned} \right\} \quad (5)$$

Where  $u$  and  $v$  are the velocity components in the  $x, y$  directions,  $\rho$  is the density of nanofluid,  $\delta$  is the

Casson fluid parameter,  $\mu$  is the dynamic viscosity of the nanofluid,  $k_r$  is the chemical reaction coefficient,  $g$  is the acceleration due to gravity,  $\beta$  and  $\beta^*$  denotes the volumetric coefficient of thermal and concentration expansion,  $\sigma$  is the electrical conductivity,  $B(x) = B_0 e^{Nx/2L}$  is the variable magnetic field,  $N$  is the exponential parameter,  $\alpha = k / (\rho c_p)$  is the thermal diffusivity,  $q_r$  is the radiative heat flux,  $D_m$  is the molecular diffusivity of species concentration,  $\sigma_1$  is the Stefan-Boltzmann constant and  $\chi$  is the mean absorption coefficient.

We now introduce the similarity variables as

$$\eta = y(U_0 / 2\nu L)^{0.5} e^{0.5Nx/L}, \quad u = U_0 e^{Nx/L} f'(\eta), \quad T = T_w = T_\infty + T_0 e^{Nx/2L} \theta(\eta),$$

$$v = -N(\nu U_0 / 2L)^{0.5} e^{0.5Nx/L} \{f(\eta) + \eta f'(\eta)\}, \quad C = C_w = C_\infty + C_0 e^{Nx/2L} \phi(\eta),$$
(6)

By making use of Eq. (6), Eqs (1)-(5) can be transformed as

$$(1 + \delta^{-1}) f''' + Nff'' + Gr\theta + Gc\phi - 2Nf'^2 - Mf' = 0,$$
(7)

$$\left(\frac{1}{Pr} + Ra\right) \theta'' + Nf\theta' + Ec(f'')^2 - 4N\theta f' = 0,$$
(8)

$$\phi'' - NSc4f'\phi + NScf\phi' - Kr\phi = 0,$$
(9)

Subject to the boundary conditions

$$f = 0, f' = 1, \theta = 1, \phi = 1 \quad \text{at } \eta = 0$$

$$f' \rightarrow 0, \theta \rightarrow 0, \phi \rightarrow 0, \quad \text{as } \eta \rightarrow \infty$$
(10)

Where  $N$  is the exponential parameter,  $Gr = 2Lg\beta T_0 / U_0^2$ ,  $Gc = 2Lg\beta^* C_0 / U_0^2$  are the thermal and mass Grashof numbers,  $M = 2L\sigma B_0^2 / \rho U_0$  is the magnetic field parameter,  $Pr = \nu / \alpha$  is the Prandtl number,  $Ra = 16\sigma_1 T_\infty^3 / 3\chi(\mu c_p)_{nf}$  is the thermal Radiation parameter,  $Ec = U_0^2 / T_0(c_p)_{nf}$  is the dissipation parameter,  $Sc = \nu / D_m$  is the Schmidt number and  $Kr = \nu k_r / U_0^2$  is the chemical reaction parameter.

The physical quantities of engineering interest, the skin friction at the surface  $C_{f_x}$ , local Nusselt number

$Nu_x$  and local Sherwood number  $Sh_x$  are given by

$$Re_x^{0.5} C_{f_x} = (1 + \delta^{-1}) f''(0),$$

$$Re_x^{-0.5} Nu_x = -\theta'(0),$$

$$Re_x^{-0.5} Sh_x = -\phi'(0),$$
(11)

where  $Re_x = \frac{u_w e^{Nx/L}}{\nu}$  is the local Reynolds number.

### 3. Results and Discussion

The system of Eqs. (7)-(9) with the boundary conditions in Eq. (10) are solved numerically using the effective Matlab package bvp5c. Here, we consider the non-dimensional parameter values as  $Gr = Gc = .5$ ,  $M = 1$ ,  $Pr = 7$ ,  $Ra = .5$ ,  $Ec = 0.1$ ,  $Sc = 0.6$ ,  $Kr = 0.2$ ,  $N = .1$ . These values are reserved as unvarying during the study.

Figs.2-4 reveals the effect of  $M$  on the flow, temperature and concentration profiles. It is found that the rising values of  $M$  suppresses the  $f'(\eta)$  and opposite behaviour is shown in  $\theta(\eta)$  and  $\phi(\eta)$ . Physically, rising values of magnetic field parameter produce the negative force to the flow is known as Lorentz force. This force has tendency to decrease the momentum boundary layer thickness. Figs. 5-7 portrays the variations in  $f'(\eta)$ ,  $\theta(\eta)$  and  $\phi(\eta)$  for various values of  $Ra$ . It is observed that an increase in  $Ra$  enhances the  $f'(\eta)$ ,  $\theta(\eta)$  and depreciate the  $\phi(\eta)$ . Generally, increasing values of radiation parameter establish to be energy move by the release of electromagnetic waves which take energy absent as the fluid flows.

Figs. 8-10 describe the enhancement in  $Gr$  leads to increases in  $f'(\eta)$  but the  $\theta(\eta)$  and  $\phi(\eta)$  are depreciate. Figs. 11-13 shows the variation of  $f'(\eta)$ ,  $\theta(\eta)$  and  $\phi(\eta)$  for various values of  $Gc$ . The result shows that increasing values of  $Gc$  enhances  $f'(\eta)$  and suppresses both  $\theta(\eta)$  and  $\phi(\eta)$ . The effect of  $Ec$  on  $f'(\eta)$  and  $\theta(\eta)$  is elaborated in Figs.14 and 15. It showed that the rising values of  $Ec$  boost up both  $\theta(\eta)$  and  $f'(\eta)$ . Rising values of dissipation parameter increases the thermal conductivity of the flow. The variation of  $\theta(\eta)$ ,  $\phi(\eta)$  and  $f'(\eta)$  against different values  $Kr$  is presented in Figs. 16-18. This agrees the general behaviour of  $Kr$  that the increase in chemical reaction depreciate the velocity and concentration boundary layer thickness. Here, we exposed that the  $\theta(\eta)$  rising and  $\phi(\eta)$ ,  $f'(\eta)$  retards for larger values of  $Kr$ . The influence of  $N$  on  $f'(\eta)$ ,  $\theta(\eta)$  and  $\phi(\eta)$  is displayed in Figs.19-21. It is found that increasing values of  $N$  depreciate  $f'(\eta)$  and opposite behaviour is shown in  $\theta(\eta)$  and  $\phi(\eta)$ . This is due to suppresses in the wall temperature during the boundary layer for positive values of  $N$ .

Tables 1 and 2 demonstrate the variation in the skin friction, local Nusselt number and local Sherwood number for Newtonian and non-Newtonian fluids. It is observed that increasing values of magnetic field parameter depreciate both heat and mass transfer rate. Growing values of radiation parameter maximize the skin friction and mass transfer rate and minimize the heat transfer rate. It is observed that friction factor and mass transfer rates are motivated with improving values of radiation, thermal Grashof number and mass Grashof number. Due to exponential parameter in the flow, we observed a decrement in the skin friction and this leads to enhance the heat and mass transfer rate.

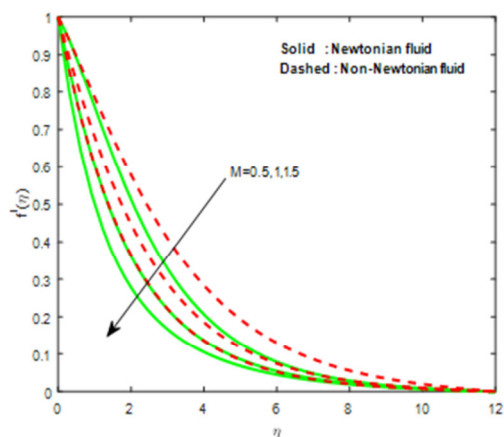


Fig. 2. Effect of  $M$  on  $f'(\eta)$ .

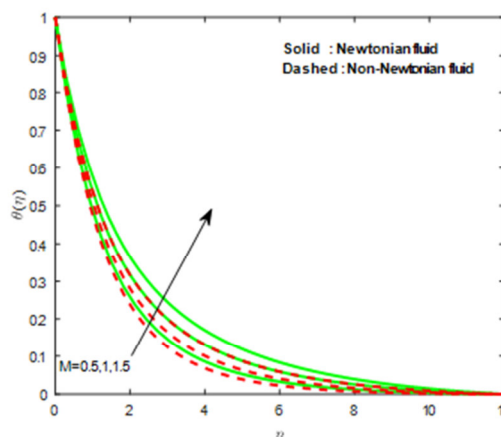


Fig. 3. Effect of  $M$  on  $\theta(\eta)$ .

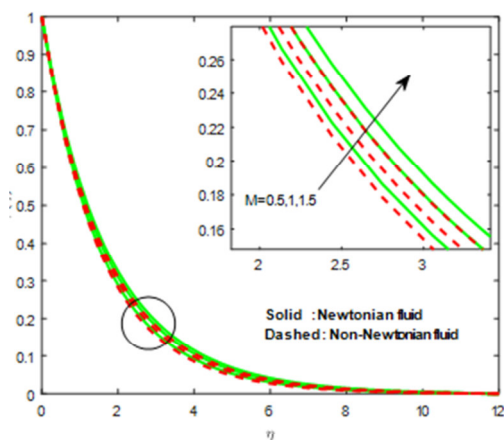


Fig. 4. Effect of  $M$  on  $\phi(\eta)$ .

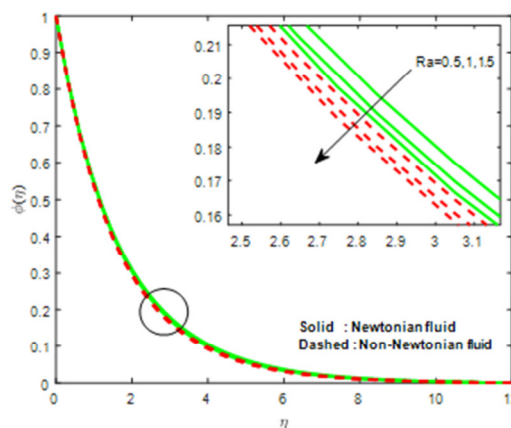


Fig. 7. Effect of  $Ra$  on  $\phi(\eta)$ .

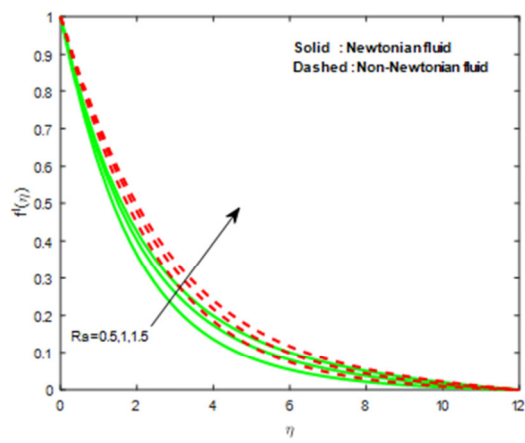


Fig. 5. Effect of  $Ra$  on  $f'(\eta)$ .

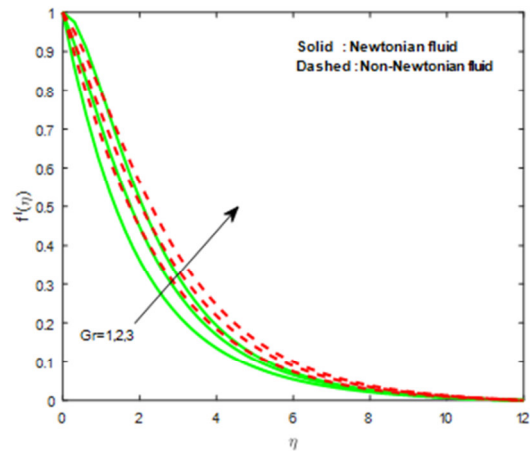


Fig. 8. Effect of  $Gr$  on  $f'(\eta)$ .

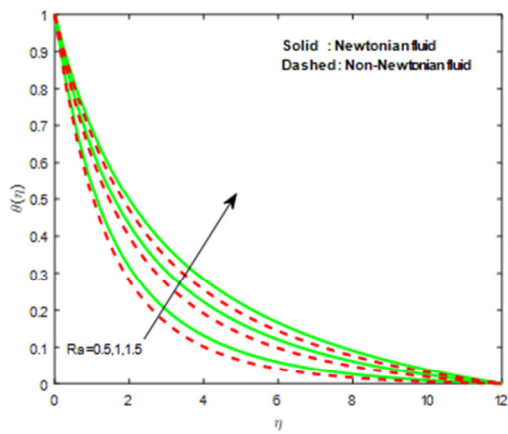


Fig. 6. Effect of  $Ra$  on  $\theta(\eta)$ .

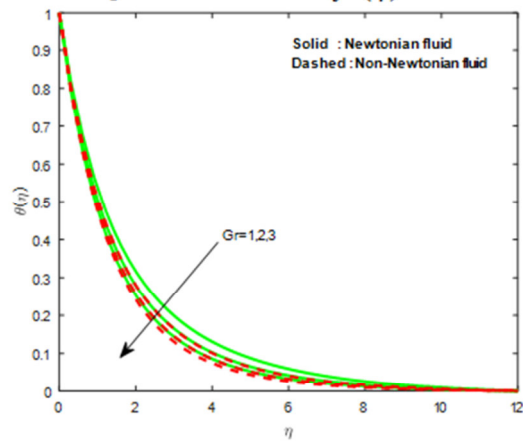


Fig. 9. Effect of  $Gr$  on  $\theta(\eta)$ .

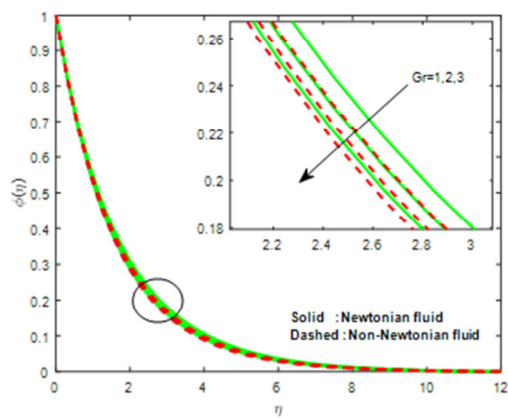


Fig. 10. Effect of  $Gr$  on  $\phi(\eta)$ .

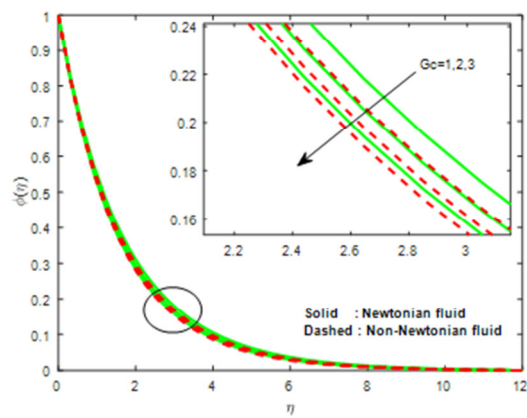


Fig. 13. Effect of  $Gc$  on  $\phi(\eta)$ .

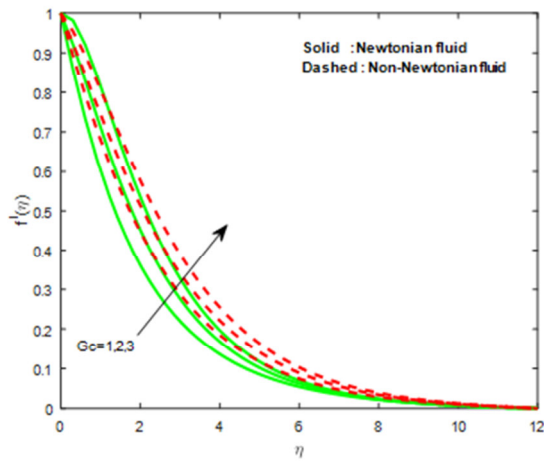


Fig. 11. Effect of  $Gc$  on  $f'(\eta)$ .

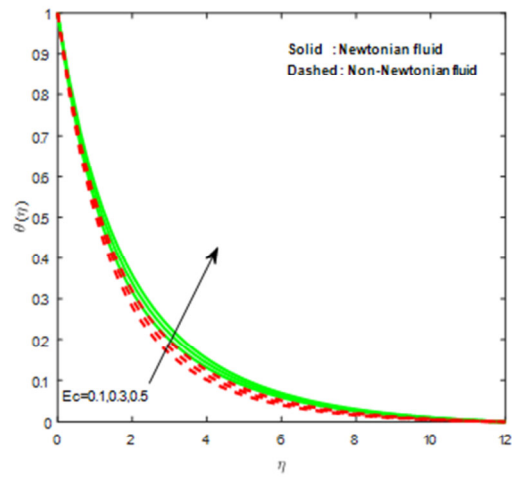


Fig. 14. Effect of  $Ec$  on  $\theta(\eta)$

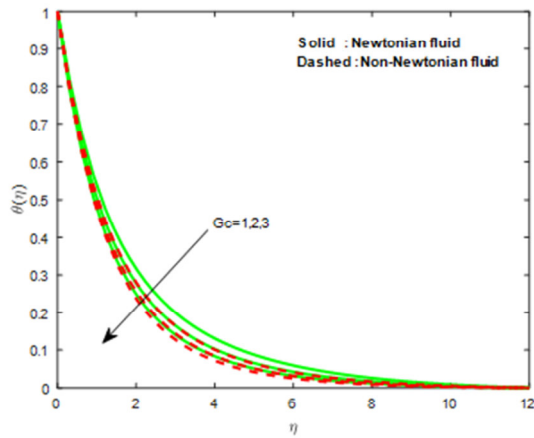


Fig. 12. Effect of  $Gc$  on  $\theta(\eta)$ .

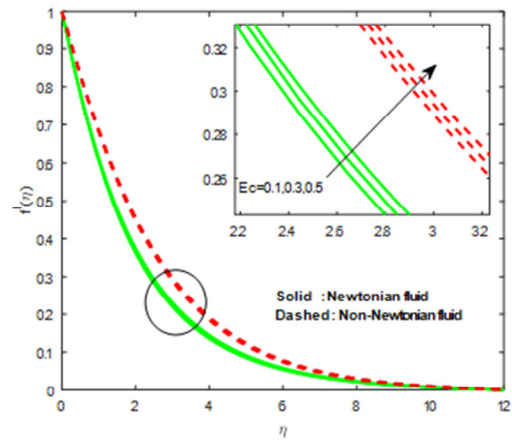


Fig. 15. Effect of  $Ec$  on  $f'(\eta)$ .

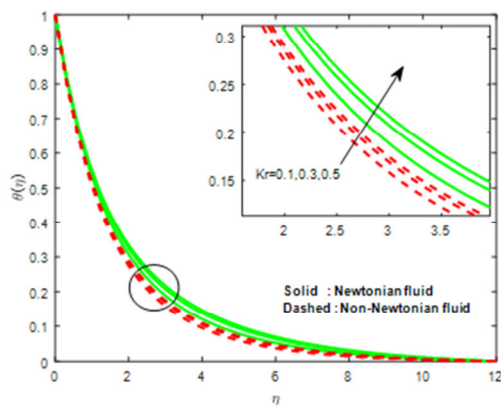


Fig. 16. Effect of  $Kr$  on  $\theta(\eta)$ .

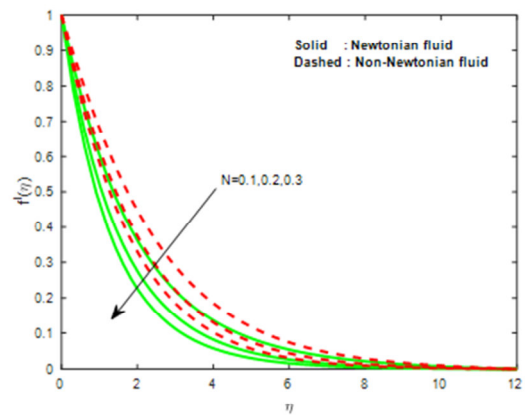


Fig. 19. Effect of  $N$  on  $f'(\eta)$ .

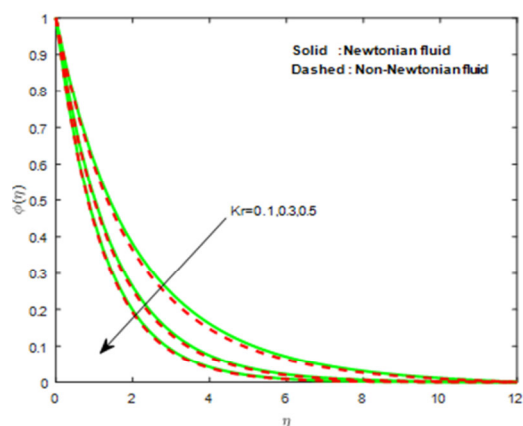


Fig. 17. Effect of  $Kr$  on  $\phi(\eta)$ .

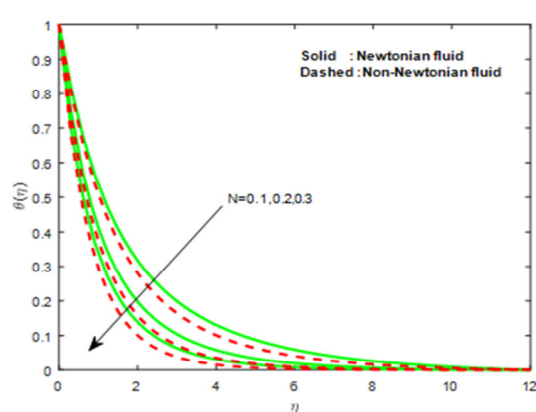


Fig. 20. Effect of  $N$  on  $\theta(\eta)$ .

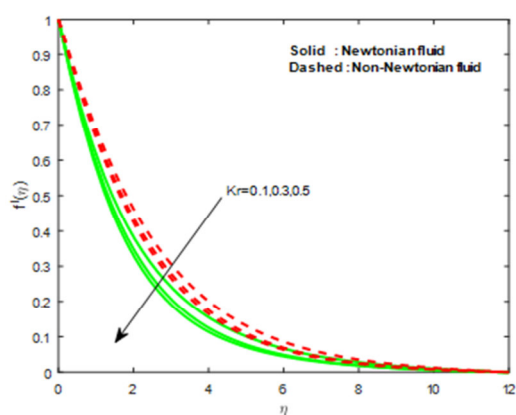


Fig. 18. Effect of  $Kr$  on  $f'(\eta)$ .

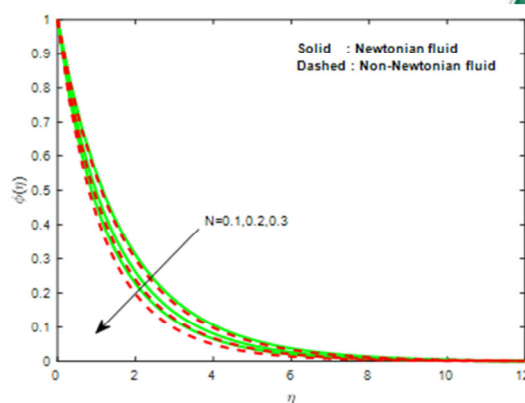


Fig. 21. Effect of  $N$  on  $\phi(\eta)$ .

**Table 1** Variations in  $f''(0)$ ,  $-\theta'(0)$  and  $-\phi'(0)$  for Newtonian fluid

$M$	$Ra$	$Gr$	$Gc$	$Ec$	$Kr$	$N$	$f''(0)$	$-\theta'(0)$	$-\phi'(0)$
0.5							-0.160105	0.752813	0.648234
1							-0.493010	0.678222	0.623839
1.5							-0.754155	0.616903	0.607050
	.5						-0.493010	0.678222	0.623839
	1						-0.461990	0.493007	0.628383
	1.5						-0.444786	0.402876	0.631012
		1					-0.493010	0.678222	0.623839
		2					-0.230151	0.729447	0.640171
		3					0.019647	0.767070	0.654264
			1				-0.493010	0.678222	0.623839
			2				-0.221864	0.731444	0.640900
			3				0.043048	0.772744	0.656527
				0.1			-0.493010	0.678222	0.623839
				0.3			-0.486490	0.631708	0.624687
				0.5			-0.480222	0.587380	0.625504
					0.1		-0.476910	0.687058	0.529891
					0.3		-0.505186	0.671925	0.703498
					0.5		-0.523354	0.663167	0.838255
						0.1	-0.493010	0.678222	0.623839
						0.2	-0.648388	0.981851	0.753429
						0.3	-0.769489	1.214644	0.862778

**Table 2** Variations in  $f''(0)$ ,  $-\theta'(0)$  and  $-\phi'(0)$  for non-Newtonian fluid

$M$	$Ra$	$Gr$	$Gc$	$Ec$	$Kr$	$N$	$f''(0)$	$-\theta'(0)$	$-\phi'(0)$
.5							-0.188074	0.765722	0.652582
1							-0.360673	0.718307	0.636042
1.5							-0.498441	0.678753	0.624002
	.5						-0.360673	0.718307	0.636042
	1						-0.339161	0.521897	0.639284
	1.5						-0.326394	0.425939	0.641284
		1					-0.360673	0.718307	0.636042
		2					-0.241681	0.745225	0.645227
		3					-0.127995	0.767211	0.653430
			1				-0.360673	0.718307	0.636042
			2				-0.235499	0.747206	0.645936
			3				-0.112850	0.771771	0.655189
				0.1			-0.360673	0.718307	0.636042
				0.3			-0.357201	0.685408	0.636547
				0.5			-0.353827	0.653649	0.637039
					0.1		-0.350029	0.723584	0.544783
					0.3		-0.368374	0.714661	0.714016
					0.5		-0.379354	0.709744	0.846692
						0.1	-0.360673	0.718307	0.636042
						0.2	-0.449090	1.043360	0.779451
						0.3	-0.516311	1.292918	0.901670

#### 4. Conclusions

This study presents the influence of magnetic field, chemical reaction, radiation, dissipation, buoyancy forces and exponential parameter on MHD flow of Casson fluid. The governing PDE's are converted to nonlinear ODE's by using similarity transformation and then numerically solved by bvp5c with Matlab package. The impact of different pertinent parameters on flow, temperature and concentration fields are analysed and existing through tables and graphs. The numerical results are summarized as follows:

- Magnetic field parameter helps to suppress the heat and mass transfer rate.
- Influence of buoyancy forces are high in Casson fluid.
- Chemical reaction parameter helps to enhance the local Nusselt and Sherwood numbers.
- Rising values of exponential parameter increases both reduced Nusselt number and Sherwood number.
- Dissipation parameter has tendency to regulate the heat transfer performance.

#### References

[1]Emad M AboEldahab, Radiation effect on heat transfer in an electrically conducting fluid at a stretching surface with a uniform free stream, J. of Physics D: Appl. Phys., 33(24) (2000).  
 [2]S. Prammanik, Casson fluid flow and heat transfer past an exponentially porous stretching sheet in presence of thermal radiation, Ain Shams Eng. J., 5 (2014) 205-212.  
 [3]A. A. Afity, the effect of radiation on free convective flow and mass transfer past a vertical isothermal cone surface with chemical reaction in the presence of a transverse magnetic field, Can. J. of Phys., 82(6) (2004) 447-458.  
 [4]I. L. Animasaun, Casson fluid flow with variable viscosity and thermal conductivity along exponentially stretching sheet embedded in a thermally stratified medium with exponentially heat generation, J. of Heat and Mass Tran. Res., 7(2) (2015) 63-78.  
 [5] S. Mukhopadhyay, MHD boundary layer flow and heat transfer over an exponentially stretching sheet embedded in a thermally stratified medium, Alex. Eng. J., 52(3) (2013) 259-265.  
 [6]M. Sajid and T. Hayat, Influence of thermal radiation on the boundary layer flow due to an exponentially stretching sheet, Int. Com. in Heat and Mass Transfer, 35(3) (2008) 347-356.  
 [7]W. Ibrahim, B. Shankar and M. M Nandeppanavar, MHD stagnation point flow and heat transfer due to nanofluids a stretching sheet, Int. j. of Heat and Mass Tran., 56(1) (2013) 1-9.  
 [8]C. S. K. Raju, N. Sandeep, V. Sugunamma, M. Jayachandra Babu and J. V. Ramana Reddy, Heat and mass



- transfer in magnetohydrodynamic Casson fluid over an exponentially permeable stretching surface, *Eng. Sci. and Tec. An Int. J.*, 19(1) (2016) 45-52.
- [9] M. R. Krishnamurthy, B. C. Prasannakumara, B. J. Gireesha and R. S. R. Gorla, Effect of chemical reaction on MHD boundary layer flow and melting heat transfer of Williamson nanofluid in porous medium, *Eng. Sci. and Tec. Int. j.*, 19 (2016) 53-61.
- [10] G. Mahanta and S. Shaw, 3D Casson fluid flow past a porous linearly stretching sheet with convective boundary condition, *Ale. Eng. J.*, 54 (2015) 653-659.
- [11] B.J. Gireesha, B. Mahanthesh, I.S. Shivamumara and K. M. Eshwarappa, Melting heat transfer in boundary layer stagnation-point flow of nanofluid toward a stretching sheet with induced magnetic field, *Eng. Sci. and Tech.an Int. J.*, 19 (2016) 313-321.
- [12] T. Hayat, M. Ljaz Khan, M. Waqas, A. Alsaedi and T. Yasmeen, Diffusion of chemically reactive species in third grade fluid flow over an exponentially stretching sheet considering magnetic field effects, *Chi. J. of Chem. Eng.*, 25(3) (2017) 257-263.
- [13] T. Hayat, M I. Khan M. Waqas, T. Yasmeen and A. Alsaedi, Viscous dissipation effect in flow of magnetonanofluid with variable properties, *J. of Mol. Liquids*, 222 (2016) 47-54.
- [14] I. L. Animasaun, E. A. Adebile and A. I. Fagbade, Casson fluid flow with variable thermo-physical property along exponentially stretching sheet with suction and exponentially decaying internal heat generation using the homotopy analysis method, *J. of Nig. Math. Soc.* 35 (2016) 1-17.
- [15] J. V. Ramana Reddy, V. Sugunamma and N. Sandeep, Dual solution for heat and mass transfer in chemically reacting radiative non-Newtonian fluid with aligned magnetic field, *J. of Naval Arc. and Marine Eng.*, 14 (2017).
- [16] T. Hayat, M. Ijaz Khan, M. Waqas, A. Alsaedi and M. Farooq, Numerical simulation for melting heat transfer and radiation effects in stagnation point flow of carbon-water nanofluid, *Com. meth. In Appl. Mech. and Eng.*, 315 (2017) 1011-1024.
- [17] S. Nadeem, R. Ul Haq, N. S. Akbar and Z. H. Khan, MHD three dimensional Casson fluid flow past a porous linearly stretching sheet, *Alex. Eng. J.*, 52(4) (2013) 577-582.
- [18] M. I. Khan, M. Waqas, T. Hayat and A. Alsaedi, Magnetohydrodynamic (MHD) stagnation point flow of Casson fluid over a stretched surface with homogeneous-heterogeneous reaction, *J. of The. and Com. Che.*, 16 (2017).
- [19] T. Hayat, M. Rashid, M. Imtiaz and A. Alsaedi, MHD effects on a thermo-solutal stratified nanofluid flow on an exponentially radiating stretching sheet, *J. of Apl. Mech. and Tech. Phy.*, 58(2) (2017) 214-223.
- [20] M. E. Ali and N. Sandeep, Cattaneo-Christov model for radiative heat transfer of magnetohydrodynamic Casson-ferrofluid: A numerical study, *Result in Physics*, 7 (2017) 21-30.
- [21] M. Sathis Kumar, N. Sandeep, B. Rushi Kumar and J. Prakash, Effect of Cattaneo-Christov heat flux on nonlinear radiative MHD flow of casson fluid induced by a semi-infinite stretching surface, *FHMT*, 8 (2017) 8.
- [22] M. Tamoor, M. Waqas, M. Ijaz Khan, A. Alsaedi and T. Hayat, Magnetohydrodynamic flow of Casson fluid over a stretching cylinder, *Result in Physics*, 7 (2017) 498-502.
- [23] G.Kumaran, N.Sandeep, M.E.Ali, Computational analysis of magneto-hydrodynamic Casson and Maxwell flows over a stretching sheet with cross diffusion, *Results in Physics*, 7 (2017) 147-155.
- [24] J.V.Ramana Reddy, V.Sugunamma, N.Sandeep, Cross diffusion effects on MHD flow over three different geometries with Cattaneo-Christov heat flux, *Journal of Molecular Liquids*, 223, 1234-1241, 2016.
- [25] M.Jayachandra Babu, N.Sandeep, Three-dimensional MHD slip flow of a nanofluid over a slendering stretching sheet with thermophoresis and Brownian motion effects, *Advanced Powder Technology*, 27, 2039-2050, 2016.
- [26] .L.Animasaun, N.Sandeep, Buoyancy induced model for the flow of 36nm alumina-water nanofluid along upper horizontal surface of a paraboloid of revolution with variable thermal conductivity and viscosity, *Powder Technology*, 301,858-867, 2016.
- [27] N.Sandeep, O.K.Koriko, I.L.Animasaun, Modified kinematic viscosity model for 3D-Casson fluid flow within boundary layer formed on a surface at absolute zero, *Journal of Molecular Liquids*, 221,1197-1206,2016.
- [28] N.Sandeep, M.S.Jagadeesh Kumar, Heat and Mass transfer in nanofluid flow over an inclined stretching sheet with volume fraction of dust and nano particles, *Journal of Applied Fluid Mechanics*, 9(5), 2205-2215, 2016.
- [29] C.Sulochana, N.Sandeep, Flow and heat transfer behavior of MHD dusty nanofluid past a porous stretching/shrinking cylinder at different temperatures, *Journal of Applied Fluid Mechanics*, 9(2), 543-553, 2016.
- [30] C.Sulochana, G.P.Aswin Kumar, N.Sandeep, Transpiration effect on stagnation-point flow of a Carreau nanofluid in the presence of thermophoresis and Brownian motion, *Alexandria Engineering Journal*, 55, 1151-1157, 2016.